GNSS orbit prediction with enhanced force model

GNSS orbit prediction with enhanced force model

Andrei Pukkila, Juha Ala-Luhtala, Robert Piché, Simo Ali-Löytty
Tampere University of Technology. Tampere, Finland
Email: andrei.pukkila@tut.fi, juha.ala-luhtala@tut.fi, robert.piche@tut.fi, simo.ali-loytty@tut.fi

***Abstract*—Orbit prediction algorithms can be used in a portable positioning device to reduce the Time to First Fix and to augment the received broadcast ephemeris. In this work, we study the two-week prediction accuracy improvement that can be obtained when adding some smaller forces to our previously developed algorithm. These forces arise from solid earth tides, relativity effect, and the gravitational pull of Venus and Jupiter. Also, a box-wing model of solar radiation pressure is considered. The new model with aforementioned extra forces is tested for GPS, GLONASS and Beidou satellites using initial conditions computed from precise ephemerides. It is found that the enhancements give small but not negligible improvement, with more accurate Sun and Moon coordinates having the most effect and relativity correction for Earth's gravity the least. However, the improvements come at the cost of noticeable increase in computational load.**

I. Introduction

A GNSS satellite's orbit can be predicted over a one or two week interval using broadcast ephemeris data. The predicted orbits can be used for example in an autonomous positioning device to reduce the Time to First Fix (TTFF) or to augment the broadcast ephemerides in difficult environments.

The accuracy of the predicted orbit depends on the quality of the force model and on the quality of the initial conditions for the satellite's position and velocity. Increasing the complexity of the force model leads to a computationally heavier algorithm, which is not desired in a portable positioning device. Therefore, a suitable compromise in between the detail of modeled forces and the accuracy must be found. Typically, the force model contains physical models for the gravitational forces of the Earth, the Sun and the Moon, and an empirical model to account for solar radiation pressure. The problem of estimating suitable initial conditions from the satellite's broadcast ephemeris is addressed in our previous publications [1], [2]. Also, for a completely autonomous prediction algorithm, we need a method in order to predict the satellite clock offsets. Details for clock offset prediction can be found from [1], [3].

In this paper, we study the effects of some smaller forces on the quality of orbit prediction. These include the tidal forces of the solid earth, relativity correction for moving satellite in Earth's gravity, and gravitational forces generated by Venus and Jupiter. A simple box-wing model was also adapted to support our SRP model. A lot of other smaller forces were also considered, but eventually neglected and judged to have no significant result in overall prediction accuracy. The effect of the additional forces on the prediction error is investigated for GPS, GLONASS and Beidou satellite systems using initial conditions computed from precise ephemerides.

978-1-4799-9858-6/15$31.00 2015 IEEE

II. Model

A. Basic equation of motion

Our model for the satellite's equation of motion is given by

$$\ddot{\mathbf{r}}_{\text{Sat}} = \mathbf{a}_{\text{Earth}} + \mathbf{a}_{\text{Sun}} + \mathbf{a}_{\text{Moon}} + \mathbf{a}_{\text{SRP}} + \mathbf{a}_{\text{unaccounted}}, \quad (1)$$

where $\mathbf{a}_{\text{Earth}}$, $\mathbf{a}_{\text{Sun}}$ and $\mathbf{a}_{\text{Moon}}$ are the accelerations caused by the gravitation of the Earth, the Sun and the Moon respectively. The fourth term $\mathbf{a}_{\text{SRP}}$ is the acceleration caused by the solar radiation pressure. The last term $\mathbf{a}_{\text{unaccounted}}$ represents the unaccounted acceleration terms which are the main topic of this research. The forces are also shown in Figure 1.

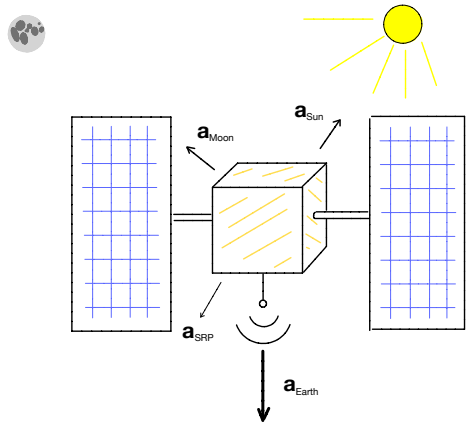

Fig. 1. The 4 main forces which contribute to satellite orbit estimation in Terrestrial Intermediate Reference System. Three largest acceleration terms are generated by gravitational effects from the Earth, Moon and Sun ($\mathbf{a}_{\text{Earth}}$, $\mathbf{a}_{\text{Moon}}$ and $\mathbf{a}_{\text{Sun}}$). Solar radiation pressure force causes the fourth major acceleration term ($\mathbf{a}_{\text{SRP}}$).

For the Earth gravity model, we use spherical harmonic expansion of the gravity potential with terms up to the degree and order 12. The values for the geopotential coefficients are obtained from the EGM2008 model [4]. The Sun and the Moon are considered as point masses. The solar radiation pressure model is of the form [5]

$$\mathbf{a}_{\text{SRP}} = \lambda \left(-\alpha_1 \frac{1}{r_{\text{sun}}^2} \mathbf{e}_s + \alpha_2 \mathbf{e}_y \right), \quad (2)$$

where r_{sun} and $\mathbf{e}_{\text{s}}$ are the distance and unit vector from the satellite to the Sun respectively. The vector $\mathbf{e}_y$ points along the satellite's solar panel axis and is given by

$$\mathbf{e}_y = \frac{\mathbf{r}_{\text{Sat}} \times (\mathbf{r}_{\text{Sun}} - \mathbf{r}_{\text{Sat}})}{\| \mathbf{r}_{\text{Sat}} \times (\mathbf{r}_{\text{Sun}} - \mathbf{r}_{\text{Sat}}) \|}. \quad (3)$$

The factor $\lambda \in [0,1]$ is a shadow factor, such that $\lambda = 1$, when the satellite is in sunlight and $\lambda = 0$, when the satellite is completely in the Earth's shadow. We have used the conical shadow model described in [6]. The parameters α_1 and α_2 are satellite-specific parameters that are estimated separately for each satellite. The parameter α_1 is a scaling parameter that is used to account for the uncertainty in the mass, surface area and reflectivity of the satellite. The parameter α_2 represents the magnitude of the y-bias acceleration. Variables $\mathbf{r}_{\text{Sat}}$ and $\mathbf{r}_{\text{Sun}}$ are vectors from the Earth's gravity center to satellite and to the Sun in Terrestrial Intermediate Reference System.

B. Improved model

In this section, we study enhancements to our existing force model terms and introduce some smaller forces previously left unaccounted. As the term $\mathbf{a}_{\text{unaccounted}}$ is constituted of several dozens of smaller separate terms, we can't include all physical forces in our model. Otherwise our orbit prediction algorithm would be computationally too heavy to run in portable devices. This study concentrated on the largest forces.

The first correction that we included was Earth's solid tides. Solid tides are the result of Earth's deformation from disturbing gravity potentials. The correction is calculated by changing the 2nd order unnormalized coefficients in the spherical harmonic expansion for the gravity potential. The normalized term changes can be calculated by

$$\left\{ \begin{array}{c} \Delta C_{2m} \\ \Delta S_{2m} \end{array} \right\} = 4k_{2,m} \left(\frac{GM}{GM_\oplus} \right) \cdot N_{nm} \left\{ \begin{array}{c} \cos(m\lambda) \\ \sin(m\lambda) \end{array} \right\}, \quad (4)$$

where

$$N_{2m} = \left(\frac{R_\oplus}{s} \right)^{n+1} \sqrt{\frac{(2+2)\,(2-m)!^3}{(2+m)!^3}} P_{2m}(\sin\phi). \quad (5)$$

Here $k_{2,m}$ represents the Love numbers and m is a gravity potential coefficient index. $R_\oplus$ and $M_\oplus$ are the distance from Earth's gravity center to satellite and Earth's mass. M and s represent the mass of disturbing object and its distance from Earth's gravity center. G is the gravity constant. Angles λ and ϕ are latitude and longitude of the satellite. The function P_{nm} is the value of Legendre polynomial of degree n and order m. This model for solid tides is given in [6] and more accurate Love number values can be found in [7]. The final step is to unnormalize the term changes [6]. It can be done with

$$\left\{ \begin{array}{c} \Delta \bar{C}_{2m} \\ \Delta \bar{S}_{2m} \end{array} \right\} = \sqrt{\frac{(2+m)!}{5 \cdot (2-\delta_{0,m})\,(2-m)!}} \left\{ \begin{array}{c} \Delta C_{2m} \\ \Delta S_{2m} \end{array} \right\}. \quad (6)$$

Here $\delta_{0,m}$ represents the Kronecker delta function which gains the value of 1 only when $m = 0$ and the value 0 otherwise.

The second correction to the force model was an additional scaling of the Earth's gravity field. The theory of general relativity states that a moving object sees the space-time surrounding it differently than a resting observer. Therefore, a moving satellite has to undergo relativistic coordinate transformation if we desire to predict the motion really accurately. Essentially, this means that the satellite experiences an increase in gravity because of the relativistic coordinate transformation. Without going further into details of general relativity, the increase in Earth's gravity for a satellite is given by [6]:

$$\Delta \mathbf{a}_{\text{Earth}} = -\frac{GM_\oplus}{r^2} \mathbf{e}_r \left(3\frac{v^2}{c^2} \right). \quad (7)$$

Here r is distance from Earth's gravity center and v is the satellite's velocity. This approximation holds rather well for all satellites on a circular orbit. Because most GNSS satellites are in a nearly circular orbit, this formula suits us well.

The third major correction that we tested was a simple version of a box-wing SRP model. We tested the correction only for GPS satellites. This correction included a semi-empirical sun-earth-satellite angle dependence in the satellite surface area. We assumed that the technical box of the satellite would rotate in relation to the Sun as it is kept directed toward Earth, while solar panels always face the Sun (with a small phase lag). The dependence was assumed to be simply of a sine form. Therefore our modified SRP model is of the form:

$$\mathbf{a}_{\text{SRP}} = \lambda \left(-A \cdot \alpha_1 \frac{1}{r_{\text{sun}}^2} \mathbf{e}_s + \alpha_2 \mathbf{e}_y \right), \quad (8)$$

where

$$A = 1 + \alpha_3 \cdot (\sin(|\gamma|) - 0.5). \quad (9)$$

Here γ represents the angle between the satellite and the Sun if observed from the gravity center of the Earth. Parameter α_3 was hand tuned by using a large number of orbit predictions. We didn't use any available box-wing models in determining the equation (9). However, it is noteworthy that certain forces in already published box-wing models [8] resemble our simplified box-wing-correction. We didn't use a previously designed box-wing corrections as they are, because most of them are computationally noticeably heavier. Even our simple correction slowed down the computation by over 10%.

The next correction in our force model was enhancing the planetary body coordinate accuracy. Our force model used a simple analytical formula to calculate the Sun and the Moon positions [6]. To improve the position accuracy, we used Jet Propulsion Lab's DE202 planetary body ephemeris [9]. The ephemeris gives planetary body coordinate data in form of Chebychev factors in pre-determined time intervals. The older DE202 ephemeris is desirable in favor of the newer DE400 series ephemerides because it doesn't require an extra coordinate transformation when used in our algorithm.

Because relativity correction for moving satellite accelerates the satellite towards the Earth and we don't have a good model for albedo that is roughly in the opposite direction, we decided to calibrate antenna thrust to roughly compensate for both Earth albedo and the actual antenna thrust. If we know the directional transmit power P of the antenna, we can calculate antenna thrust with formula

$$\mathbf{a}_{\text{ant}} = \frac{\mathbf{F}}{m} = \frac{d\mathbf{p}}{dt} \cdot \frac{1}{m} = -\frac{P}{mc} \cdot \frac{\mathbf{r}_{sat}}{||\mathbf{r}_{sat}||}. \quad (10)$$

Here m is the satellite's mass, $\mathbf{F}$ is the antenna thrust force, $\mathbf{p}$ is the total momentum of the emitted photons and c is the speed of light.

C. Unaccounted Forces

The largest force that we didn't consider fully was Earth's albedo. However, as previously mentioned, we calibrated antenna thrust to roughly match a constant albedo. In future work it would be good to estimate albedo as time and angle - dependent force and try to build sufficiently lightweight model for it to be used in portable devices. Previous research like [10] should be consulted in such undertaking.

During the research, we also tested briefly several other smaller forces. The maximum accelerations caused by these forces vary in the range of $10^{-9} - 10^{-12} \frac{\mathrm{m}}{\mathrm{s}^2}$. These forces included: relativity correction for satellite moving in the Sun's gravity and redshift-blueshift SRP corrections for moving satellite. A moving satellite also experiences change in SRP force direction because of relativity and specifically aberration of electromagnetic radiation. The Sun's radiation power also changes a little bit over time, but that was not taken into account in our orbit predictor.

It is also noteworthy to realize that satellite emits a lot of infrared radiation and some of this radiation may be directional and dependent on satellite's attitude [11]. More accurate radiation pressure models would also need to consider this. The emitted infrared radiation becomes especially influential for satellite orbit prediction when the satellite passes behind the Earth's shadow. This is due to the fact that the satellite does not cool down instantly after passing into the shadow nor does it heat up instantly after it leaves the Earth's shadow. According to our tests, some satellites behave better with our current force model than others in the case of entering and leaving Earth's shadow.

D. Reference frames

A satellite's position is usually reported in an Earth-fixed, Earth-centered (ECEF) reference frame. An ECEF system has its origin at the mass center of the Earth and its axes are fixed with respect to the Earth's surface. However, the integration of the satellite's equation of motion has to be done in an inertial reference frame. An inertial reference system maintained by the IERS is the Celestial Reference System (CRS). CRS is a reference system whose origin is in the center of the Earth and whose coordinate axes maintain their orientation with respect to distant stars. Instead of using the CRS system directly as an inertial reference frame, we have adopted the use of the Terrestrial Intermediate Reference System (TIRS) at epoch t_0, where t_0 is the initial time of prediction. The use of this intermediate reference system allows computationally lighter transformation between ECEF and inertial frames when we neglect the small change in precession and nutation during the relatively short prediction intervals. More details about the transformation matrices can be found in [1].

III. Results

The quality of the satellite's initial position and velocity are crucial for good orbit prediction accuracy. For example, a GPS satellite travels roughly $3 \frac{\mathrm{km}}{\mathrm{s}}$. If the initial velocity has an error of $0.3 \frac{\mathrm{mm}}{\mathrm{s}}$ (one ten-millionth of the satellite's speed), prediction will be off by more than a one meter after just a single hour. That is why we decided to use precise ephemerides.

Altogether, we calculated well over 4000 years worth of orbit predictions to get accurate enough statistics.

The SISRE (Signal-In-Space-Range-Error) describes how GNSS satellite location and clock errors contribute in pseudorange standard deviation. SISRE can be approximated with formula [1], [12], [13]:

$$\sigma_{\mathrm{SISRE,GPS}} = \sqrt{a\sigma^2_{\Delta R - c\Delta t} + \frac{1}{b}(\sigma^2_{\Delta T} + \sigma^2_{\Delta N})}. \qquad (11)$$

Here, the parameter $\sigma_{\Delta R - c\Delta t}$ represents the standard deviation of radial and clock errors. Parameters $\sigma_{\Delta T}$ and $\sigma_{\Delta T}$ are transverse and normal component standard deviations. Parameters a and b are orbit-specific and are found in table I.

TABLE I
SISRE PARAMETERS [1], [12], [13] FOR FORMULA (11)

	GPS	GLONASS	BDS/MEO	BDS/IGSO,GEO
a	1	0.98	0.98	0.99
b	49	45	54	127

SISRE roughly also describes end user's positioning error, but for this use SISRE error would also need to be factored with GDOP (Geometric-Dilution-Of-Precision).

A. GPS

The GPS system is the oldest and most popular GNSS system currently in use. Its satellites have undergone several generations and technology has matured during last decades. We decided to use precise ephemeris data for the year 2012 from NGA to evaluate our force model. The GPS satellites that didn't have the entire year worth of precise ephemeris data were left out from the tests. These satellites included the ones that were either launched or decommissioned during the year.

The tests were run separately for each force model addition. For each satellite, we run 350 orbit predictions, each 14 days in length with initial times spanning the whole year 2012.

In Figure 2, we see the GPS orbit prediction results for the satellite that showed the best improvement.

As we can see, enhancements in the force model are quite visible in the best case scenarios. Especially using DE202 data for the Sun and Moon positions seems to be an important addition. For short term predictions (0-2 days), the results are improved by 30% on average. With longer predictions, the accuracy starts to deteriorate. Only few GPS satellites get over 10% improvement on average from the enhanced force model, if prediction length is as long as 14 days.

In general the two most important additions for the force model seem to be: using the DE202 ephemeris for Sun and Moon coordinate calculations and box-wing SRP addition. Solid tide correction for Earth's gravity seems to help systematically too, but not as much. Relativity correction is not showing much improvement either. We believe that relativity correction would be important if we were to implement a better Earth albedo force into our force model.

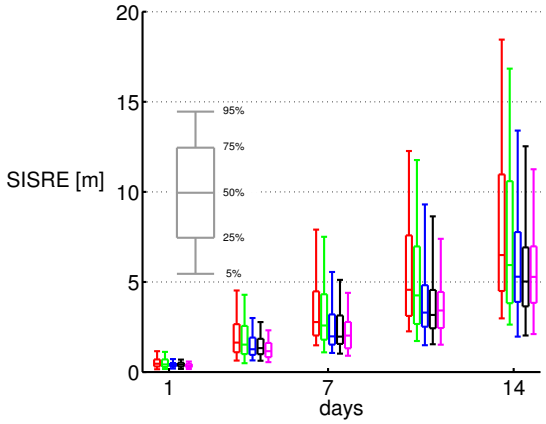

Fig. 2. Orbit prediction results for GPS satellite PRN14. The corrections are added from left to right, each new correction also including all the previous corrections. Old force model (red), solid tide correction (green), DE202 Sun and Moon coordinates (blue), relativity correction for Earth's gravity and antenna thrust (black) and box-wing SRP adaptation (magenta).

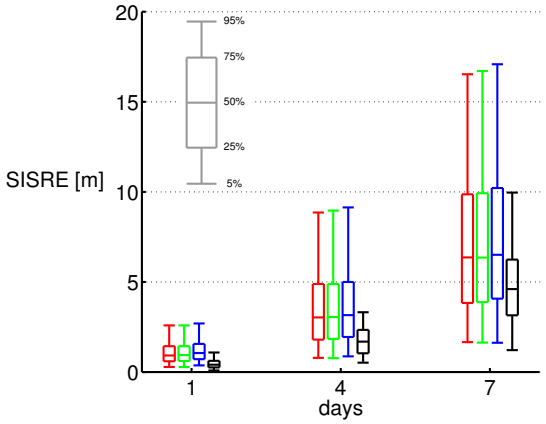

Fig. 3. Orbit prediction results for Beidou satellite PRN7 in IGSO orbit. The corrections are added from left to right, each new correction also including all the previous corrections. Old force model (red), solid tide correction (green), relativity correction for Earth's gravity and antenna thrust (blue) and DE202 Sun and Moon coordinates (black).

B. GLONASS

GLONASS is the second GNSS system to reach worldwide coverage. We used the IGS precise ephemeris data for tests. As this ephemeris data not include satellite velocities, we estimated initial velocity by minimizing the prediction error between two consecutive precise error positions. Because the results with GLONASS satellites resemble the results with Beidou MEO and IGSO satellites, we omit GLONASS here altogether.

C. Beidou

Beidou system is fully functional in Asia and China has promised to increase its coverage to the whole world by 2020. We used Wuhan University's precise ephemeris data to get satellite locations, but this data has some gaps in it. We were able to fill some of the gaps with GFZ precise ephemeris data.

The results for IGSO Beidou satellite are shown in Figure 3. Because Beidou satellites undergo more orbit corrections with their thrusters and our force model has no information about thruster usage, we concentrated only on shorter 7 day predictions to be able to have more viable predictions in our statistics. If we had used longer 14 day predictions, we would have needed to discard considerable amount of them.

As we can see, the only improvement that really affects the results visibly is DE202 ephemeris data for Sun and Moon position calculations. This seemed to be true for all GNSS satellites that were tested during this research.

Figure 4 shows the results with Beidou satellite 4 in geostationary orbit. Again, the only correction that shows any improvement is using DE202 ephemeris.

D. Force model enhancements and RTN error.

Figures 5-7 show the GPS orbit prediction errors in the RTN (Radial, Tangential, Normal) coordinate frame. The results are shown for GPS, but other tested satellites behave similarly.

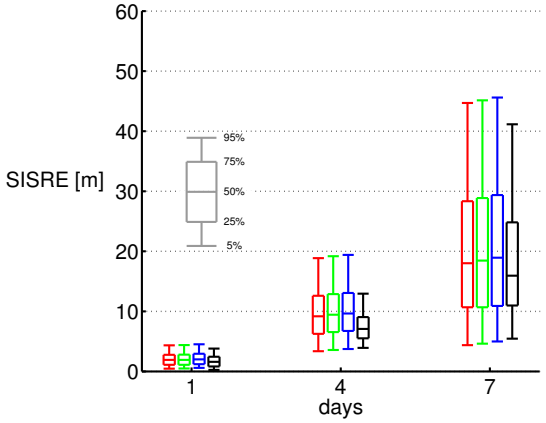

Fig. 4. Orbit prediction results for Beidou satellite PRN4 in GEO orbit. The corrections are added from left to right, each new correction also including all the previous corrections. Old force model (red), solid tide correction (green), relativity correction for Earth's gravity and antenna thrust (blue) and DE202 Sun and Moon coordinates (black).

Figure 5 shows the radial error, namely error in distance from Earth's gravity center.

We can clearly see that all other enhancements have small impact on radial error, but relativity correction doesn't seem to be of any use.

The tangential or transverse error is shown in Figure 6.

As we can see, solid tides and relativity correction do not to help much. Other enhancements in the force model are helping in reducing the satellite drift in the orbit track direction.

Using DE202 data for the Moon and Sun location calculations improves accuracy very clearly. Almost every satellite seems to be halving their normal error that accumulates during predictions. Solid tide code also shows visible results.

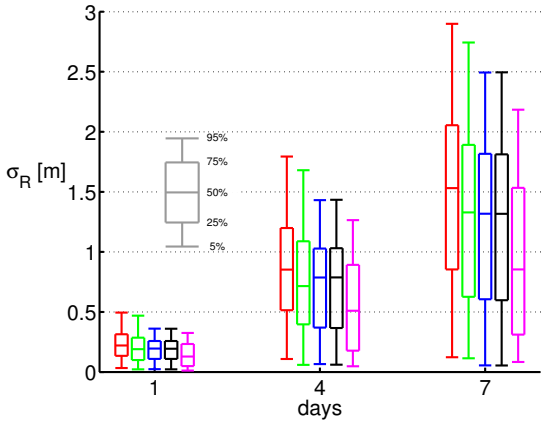

Fig. 5. Orbit prediction results for GPS satellite PRN13. The corrections are added from left to right, each new correction also including all the previous corrections. Old force model (red), solid tide correction (green), DE202 Sun and Moon coordinates (blue), relativity correction for Earth's gravity and antenna thrust (black) and box-wing SRP adaptation (magenta).

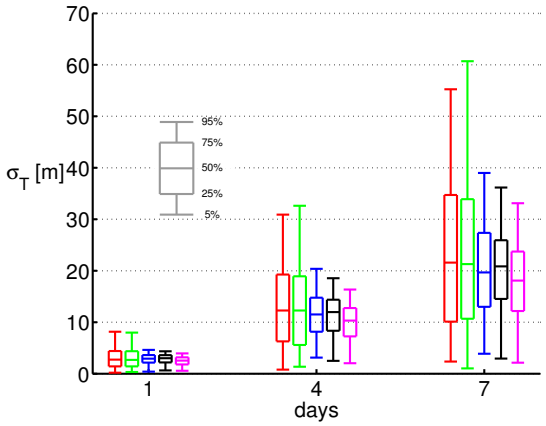

Fig. 6. Orbit prediction results for GPS satellite PRN13. The corrections are added from left to right, each new correction also including all the previous corrections. Old force model (red), solid tide correction (green), DE202 Sun and Moon coordinates (blue), relativity correction for Earth's gravity and antenna thrust (black) and box-wing SRP adaptation (magenta).

IV. Conclusions and Discussion

All the added force model corrections are orders of magnitude smaller than empirically determined SRP blackbox acceleration. For this reason, the corrections studied here were not expected to have a significant impact on overall prediction accuracy, and the results confirm this. This research used precise ephemerides in calculating satellite orbit predictions. In practical applications this wouldn't be plausible because only broadcast ephemerides are available in realtime. However, we believe that the relative effects of the model changes on prediction accuracy would be similar.

Overall, the modification that had the largest impact was the use of more accurate Sun and Moon coordinates. The results from our box-wing SRP adaptation tests lead us to

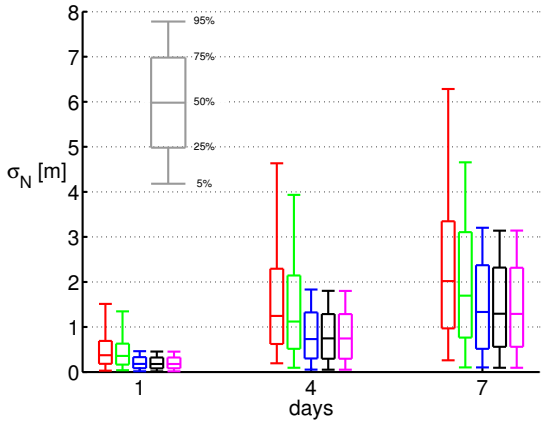

Fig. 7. Orbit prediction results for GPS satellite PRN13. The corrections are added from left to right, each new correction also including all the previous corrections. Old force model (red), solid tide correction (green), DE202 Sun and Moon coordinates (blue), relativity correction for Earth's gravity and antenna thrust (black) and box-wing SRP adaptation (magenta).

conclude that improving SRP model can also yield better results. Enhancing SRP model can easily lead to significant decrease in computation speed and therefore it should be done cautiously. The next phase in implementing the box-wing-correction further would be building a suitable estimator algorithm that would require less computing power when estimating α_3 -parameters.

For some unknown reason, our prediction algorithm does not work reliably for geostationary satellites. It is possible that either our estimates for solar radiation pressure parameters are slightly incorrect or that we would need to have a better Earth albedo model. Another possibility is that the solar radiation pressure parameters have a strong time dependence that would need to be taken into account. Gravitational forces from Jupiter and Venus often brought slight differences in the end result accuracy, but taking those forces into account yielded no overall improvements with any GNSS satellite system.

Overall, the studied enhancements in the force model seem to make a significant impact on short term (0-2 days) predictions, but long term (7-14 days) prediction accuracy often deteriorates from satellite drift in the transverse direction.

V. Acknowledgements

This research was supported by Microsoft. J. Ala-Luhtala received financial support from the Tampere University of Technology Doctoral Programme in Engineering and Natural Sciences.

References

[1] M. Seppänen, J. Ala-Luhtala, R. Piché, S. Martikainen, and S. Ali-Löytty, "Autonomous prediction of GPS and GLONASS satellite orbits," *NAVIGATION*, vol. 59, no. 2, pp. 119–134, 2012.

[2] J. Ala-Luhtala, M. Seppänen, S. Ali-Löytty, R. Piché, and H. Nurminen, "Estimation of initial state and model parameters for autonomous GNSS orbit prediction estimation of initial state and model parameters for autonomous GNSS orbit prediction," in *International Global Navigation Satellite Systems Society Symposium 2013 (IGNSS2013)*, Gold Coast, Queensland, Australia, July 2013.

[3] S. Martikainen, R. Piché, and S. Ali-Löytty, "Outlier-robust estimation of GPS satellite clock offsets," in *International Conference on Localization and GNSS*, Starnberg Germany, June 2012, pp. 1–5. [Online]. Available: http://URN.fi/URN:NBN:fi:tty-201310311406

[4] NGA. EGM2008 model coeffcients. [Online]. Available: http://earth-info.nga.mil/GandG/wgs84/gravitymod/egm2008/first_release.html

[5] J. Ala-Luhtala, M. Seppänen, and R. Piché, "An empirical solar radiation pressure model for autonomous GNSS orbit prediction," in *Proceedings of PLANS 2012 IEEE/ION Position Location and Navigation Symposium*, April 2012, pp. 568–575. [Online]. Available: http://URN.fi/URN:NBN:fi:tty-201311011414

[6] O. Montenbruck and E. Gill, *Satellite Orbits: Models, Methods and Applications*, 3rd ed. Springer, 2005.

[7] (2010) IERS technical note 36. [Online]. Available: http://www.iers.org/IERS/EN/Publications/TechnicalNotes/tn36.html

[8] P. S. C.J. Rodriguez-Solano, U. Hugentobler, "Adjustable box-wing model for solar radiation pressure impacting GPS satellites," *Advances in Space Research*, 2012.

[9] Description of JPL solar system ephemeris. [Online]. Available: http://www.cv.nrao.edu/~rfisher/Ephemerides/ephem_descr.html#ref8

[10] P. S. C. J. Rodriguez-Solano, U. Hugentobler, "Impact of albedo radiation on GPS satellites," Institute for Astronomical and Physical Geodesy, Tech. Rep., 2009.

[11] D. Vokrouhlicky and P. Farinella, "Thermal force effects on slowly rotating, spehrical artificial satellites - II. earth infrared heating," *Planet. Space Sci.*, vol. 45, no. 4, pp. 419–425, 1997.

[12] *Statistical Characterization of GLONASS Broadcast Clock Errors and Signal-In-Space Errors*, 2012. [Online]. Available: http://waas.stanford.edu/papers/Heng_IONITM_2012_StatAnalofGlonassClockAndSISErrors_Paper.pdf

[13] H. W. Jiadong Sun, Wenhai Jiao, Ed., *China Satellite Navigation Conference (CSNC) 2013 Proceedings*. Springer Heidelberg New York Dordrecht London, 2013.

APPENDIX

The table below shows approximated computational time increases for predicting the orbits of entire GPS constellation. Notice that DE202 and Solid tide corrections do not need to be calculated separately for each satellite.

TABLE II
TIME INCREASE ESTIMATED FOR 32 SATELLITE CONSTELLATION.

Force model	Extra load
DE202	5%
Solid Tide	5%
Relativity	3%
Antenna thrust	0%
Box-wing SRP	7%
TOTAL	20%

Here we also present tables of orbit prediction confidence intervals. The first table is for GPS, the 2nd is for GLONASS and the last one for Beidou. The tables display the SISRE confidence intervals of each satellite after prediction. The leftmost columns represent the results with old force model (Old). Each next column make 1 addition into the force model. Tested corrections: solid tides (+Ti), Moon and Sun positions from DE202 (+DE), antenna thrust and Relativity correction for Earth's gravity (+A,R), box-wing adaptation (+Bw.) and Planetary gravities from Jupiter and Venus (+Pl.). The last columns have a percent number that represents the total change in accuracy with all enhancements in use.

The last row represents the average value changes with entire constellation. Blue and red colors in the table note over 5% changes in accuracy.

For comprehensive collection of orbit prediction tables, one can look *http://tut.fi/posgroup/* and see MSc thesis by first author of this research. The tables are in appendix section.

TABLE III
GPS SATELLITE PREDICTIONS FOR 1 DAY.

		Confidence interval of 50%							Confidence interval of 95%						
	Typ	Old	+Ti	+DE	+A,R	+Bw.	+Pl.	TOT	Old	+Ti	+DE	+A,R	+Bw.	+Pl.	TOT
2	R	0.69	0.67	0.53	0.55	0.56	0.54	-21%	1.35	1.31	1.23	1.21	1.19	0.99	-27%
3	A	0.51	0.50	0.43	0.42	0.33	0.26	-49%	1.13	1.01	0.72	0.72	0.68	0.65	-43%
4	A	0.61	0.59	0.49	0.48	0.43	0.39	-36%	1.25	1.25	0.95	0.96	0.92	0.84	-33%
5	RM	0.55	0.51	0.45	0.44	0.44	0.44	-19%	1.14	1.06	0.83	0.82	0.82	0.82	-27%
6	A	0.50	0.50	0.43	0.42	0.36	0.30	-40%	1.10	1.01	0.71	0.72	0.66	0.64	-42%
7	RM	0.43	0.40	0.38	0.37	0.34	0.41	-4.6%	1.21	1.11	0.57	0.58	0.56	0.62	-49%
9	A	0.52	0.53	0.50	0.51	0.50	0.46	-13%	0.98	1.00	0.78	0.83	0.83	0.95	-3.1%
10	A	0.48	0.44	0.41	0.39	0.36	0.34	-30%	1.01	1.01	0.68	0.74	0.70	0.69	-32%
11	R	0.51	0.51	0.38	0.39	0.39	0.40	-23%	0.95	0.99	0.70	0.71	0.71	0.71	-25%
12	RM	0.53	0.54	0.47	0.48	0.48	0.48	-10%	1.27	1.25	0.90	0.92	0.92	0.92	-27%
13	R	0.50	0.46	0.48	0.48	0.41	0.39	-23%	1.18	1.16	0.70	0.67	0.60	0.64	-45%
14	R	0.46	0.42	0.39	0.41	0.33	0.37	-18%	1.11	1.11	0.71	0.68	0.58	0.62	-44%
15	RM	0.41	0.40	0.30	0.33	0.30	0.34	-17%	1.10	1.09	0.74	0.73	0.68	0.69	-37%
16	R	0.45	0.43	0.38	0.37	0.42	0.56	22%	1.37	1.24	0.70	0.68	0.71	0.80	-41%
17	RM	0.64	0.67	0.61	0.58	0.54	0.56	-12%	1.35	1.37	1.23	1.19	1.22	1.41	4.3%
18	R	0.63	0.60	0.58	0.55	0.51	0.56	-11%	1.22	1.17	0.93	0.96	0.95	1.13	-7.5%
19	R	0.67	0.59	0.52	0.51	0.54	0.53	-22%	1.27	1.34	1.08	1.07	1.03	0.84	-34%
20	R	0.62	0.60	0.56	0.57	0.48	0.48	-22%	1.16	1.14	0.88	0.87	0.88	1.08	-7.1%
21	R	0.74	0.70	0.55	0.55	0.56	0.53	-29%	1.68	1.58	1.27	1.30	1.28	1.17	-30%
22	R	0.54	0.50	0.44	0.44	0.38	0.41	-23%	1.07	1.09	0.87	0.88	0.92	1.11	4.0%
23	R	0.43	0.43	0.42	0.44	0.37	0.36	-18%	1.24	1.24	0.65	0.66	0.60	0.63	-49%
26	A	0.51	0.50	0.40	0.42	0.37	0.36	-29%	1.12	1.02	0.67	0.66	0.63	0.64	-42%
28	R	0.61	0.60	0.48	0.46	0.44	0.52	-15%	1.33	1.27	1.21	1.16	1.14	1.23	-8.1%
29	RM	0.59	0.58	0.46	0.47	0.47	0.47	-21%	1.35	1.34	1.18	1.17	1.17	1.17	-13%
30	A	0.63	0.58	0.49	0.49	0.43	0.36	-43%	1.09	1.09	0.87	0.82	0.78	0.78	-29%
31	RM	0.45	0.43	0.37	0.36	0.30	0.31	-32%	1.23	1.25	0.88	0.94	0.93	1.00	-19%
32	A	0.51	0.46	0.42	0.42	0.42	0.42	-18%	0.93	0.91	0.69	0.74	0.74	0.74	-20%
	AV	0.46	-4.1%	-13%	0.1%	-6.7%	0.5%	-22%	1.01	-2.4%	-26%	0.5%	-2.4%	3.0%	-27%

TABLE IV
GLONASS SATELLITE PREDICTIONS FOR 1 DAY.

		Confidence interval of 50%					Confidence interval of 95%				
	Typ	Old	+Ti	+A,R	+DE	TOT	Old	+Ti	+A,R	+DE	TOT
1	M	0.86	0.87	0.87	0.82	-5.3%	1.54	1.52	1.52	1.43	-7.1%
2	M	0.85	0.83	0.85	0.82	-3.9%	1.50	1.43	1.44	1.29	-14%
3	M	1.50	1.42	1.45	1.41	-5.7%	2.35	2.31	2.32	2.18	-7.2%
4	M	0.62	0.61	0.62	0.55	-11%	1.25	1.23	1.27	1.02	-18%
5	M	0.91	0.92	0.93	0.90	-1.2%	1.57	1.54	1.52	1.39	-11%
6	M	1.05	1.01	1.03	0.99	-5.9%	1.67	1.61	1.62	1.50	-11%
7	M	1.10	1.06	1.09	1.10	-0.5%	1.81	1.74	1.76	1.66	-8.1%
8	M	0.87	0.87	0.88	0.83	-5.2%	1.59	1.52	1.49	1.47	-7.5%
9	M	0.56	0.56	0.56	0.57	1.8%	1.19	1.22	1.19	1.10	-7.9%
10	M	0.63	0.60	0.62	0.55	-12%	1.15	1.17	1.19	1.02	-12%
11	M	0.68	0.68	0.68	0.67	-2.0%	1.45	1.44	1.48	1.32	-8.6%
12	M	0.65	0.65	0.66	0.62	-4.3%	1.22	1.22	1.25	1.06	-14%
13	M	0.61	0.62	0.63	0.57	-6.7%	1.16	1.15	1.19	1.07	-7.6%
14	M	0.64	0.63	0.62	0.58	-9.0%	1.22	1.26	1.21	1.12	-7.6%
15	M	0.57	0.57	0.58	0.52	-9.0%	1.15	1.17	1.15	0.97	-16%
16	M	0.62	0.63	0.64	0.60	-3.7%	1.24	1.19	1.21	1.03	-17%
17	M	0.68	0.63	0.65	0.60	-11%	1.42	1.42	1.48	1.36	-4.3%
18	M	0.52	0.51	0.51	0.44	-15%	1.23	1.15	1.20	0.99	-20%
19	M	0.51	0.51	0.51	0.41	-20%	1.16	1.09	1.11	1.01	-14%
20	M	0.67	0.63	0.66	0.57	-15%	1.33	1.32	1.36	1.07	-20%
21	M	0.58	0.58	0.60	0.51	-11%	1.31	1.26	1.27	1.11	-15%
22	M	0.51	0.53	0.53	0.46	-9.2%	1.24	1.18	1.23	0.96	-23%
23	M	0.52	0.50	0.51	0.44	-16%	1.23	1.20	1.24	1.00	-18%
24	M	0.54	0.53	0.53	0.45	-16%	1.25	1.20	1.24	1.08	-14%
	AV	0.72	-1.8%	1.7%	-7.2%	-7.4%	1.39	-2.1%	1.2%	-11%	-12%

TABLE V
BEIDOU SATELLITE PREDICTIONS FOR 1 DAY.

		Confidence interval of 50%					Confidence interval of 95%				
	Typ	Old	+Ti	+A,R	+DE	TOT	Old	+Ti	+A,R	+DE	TOT
1	GEO	4.14	4.19	4.22	3.90	-5.9%	7.71	7.75	7.78	7.38	-4.3%
2	GEO	3.35	3.32	3.27	2.83	-15%	8.51	8.50	8.49	8.24	-3.1%
3	GEO	5.84	5.85	5.87	5.49	-5.9%	10.2	10.2	10.2	9.85	-3.3%
4	GEO	4.58	4.61	4.65	4.50	-1.8%	7.80	7.84	7.90	7.21	-7.6%
5	GEO	4.12	4.10	4.07	3.53	-14%	7.50	7.47	7.44	6.65	-11%
6	IGSO	1.05	1.06	1.09	0.75	-28%	2.74	2.73	2.73	1.32	-52%
7	IGSO	0.89	0.90	0.94	0.35	-60%	2.31	2.34	2.38	1.04	-55%
8	IGSO	0.85	0.84	0.83	0.49	-42%	2.11	2.08	2.10	1.20	-43%
9	IGSO	0.99	0.99	0.99	0.68	-31%	2.54	2.52	2.52	1.69	-33%
10	IGSO	0.84	0.84	0.85	0.34	-60%	2.21	2.24	2.21	1.09	-51%
11	MEO	0.50	0.49	0.51	0.37	-26%	1.37	1.39	1.40	0.93	-32%
12	MEO	0.46	0.47	0.47	0.32	-31%	1.36	1.33	1.35	0.87	-36%
13	MEO	0.61	0.56	0.59	0.48	-22%	1.47	1.35	1.41	0.94	-36%
14	MEO	0.56	0.56	0.58	0.38	-32%	1.48	1.41	1.46	1.02	-31%
	AV	2.06	-0.0%	0.5%	-16%	-15%	4.23	-0.2%	0.4%	-17%	-17%